# Numerical simulation of parametrically forced gravity waves in a circular cylindrical container

**D Krishnaraja and S P Das***

Department of Mechanical Engineering, Indian Institute of Technology Madras, Chennai 600036, India

E-mail: *spdas@iitm.ac.in

**Abstract**: Parametrically forced gravity waves in axisymmetric mode in a circular cylinder filled with FC-72 with large liquid depth have been studied numerically. The instability threshold and wave breaking thresholds are plotted from the simulated results which show good agreement with the reported experimental and theoretical results. A notable observation is the presence of different time scales of wave amplitude modulations at different regimes. The wave amplitude response exhibits amplitude modulations, period tripling and period quadrupling without breaking of waves. Inertial collapse of the wave trough causes a high velocity jet ejection has also been observed when forcing amplitude crosses the breaking limit.

## 1. Introduction

Parametrically forced surface waves commonly known as Faraday waves, can be generated by shaking a container vertically inducing oscillation to the interface of two fluids. The Faraday waves have been extensively studied over many decades. Beyond a certain threshold the interface behaviour changes and even leads to various patterns depending on the type of induced vibration. Faraday noticed the waves formed at the interface have half the forcing frequency. This had been confirmed by the Rayleigh through his experiments. Benjamin & Ursell [1] put forward the first theoretical analysis of Faraday waves by carrying out a linear analysis and compared the evolution equation of amplitude to Mathieu Equation. Miles [2] developed a Lagrangian-Hamiltonian formulation to explain the weakly nonlinear surface waves in cylindrical containers. The analytical phase diagram developed based on this theory shows a good agreement with the experimental results.

Large amplitude parametrically forced gravity waves have been investigated by many researchers independently and they observed the period tripling and breaking [3-5]. The different depth ratios, tank base dimensions and its effect in non-linearity have also been investigated [6-7]. Das and Hopfinger [5] experimentally investigated the axisymmetric mode wave motion for parametrically forcing a circular cylinder with different working fluids and determined the stability threshold. They observed period tripling event near the breaking and different time scales of wave amplitude modulations. They reported wave amplitude modulations by period tripling for particular forcing amplitude at a given frequency. Near the resonance they also observed different type of stability behaviour of the wave motion (both subcritical and super-critical). There are also pattern formation studies available in literature at different frequencies [8]. They numerically investigated the dynamics of faraday waves using finite difference method. They reproduced the hexagonal and square patterns using their numerical method for tracking

Content from this work may be used under the terms of the Creative Commons Attribution 3.0 licence. Any further distribution of this work must maintain attribution to the author(s) and the title of the work, journal citation and DOI.
Published under licence by IOP Publishing Ltd

the oscillating interface. The most extensive numerical simulations have been that of Chen and Wu [9] about the nonlinear faraday waves and hysteresis.

In the present paper we focus our study on the axisymmetric mode of wave motion when a circular cylindrical container is forced with parametrically forced gravity waves. We have numerically simulated the flow with single frequency excitation and obtained the stability thresholds. We have also identified different regimes where we observed various time scales. The coexistence of different modes are also observed (neighbouring modes).

## 2. Theoretical background

The expression for natural frequency of different wave modes for a circular cylinder is developed by Miles (1984) and the dispersion relationship is given by

$$\omega_{mn} = gk_{mn}\left(1+\frac{k_{mn}^2\sigma}{g\rho}\right)\tanh\left(k_{mn}h\right)$$

The boundary condition for the container wall, $\frac{\partial\phi}{\partial r}_{r=R} = J_m^{'}\left(k_{mn}R\right)=0$ where $\phi$ is the velocity potential, with axisymmetric modes m=0, n=1 and n=2, $k_{01}R$=3.8317 and $k_{02}R$=7.0156. The asymmetric modes $k_{11}R$=1.841, $k_{21}R$=3.054, $k_{31}R$=4.201, $k_{41}R$=5.318, $k_{12}R$=5.331. The infinite fluid depth limit corresponds to $\tanh\left(k_{mn}h\right)=1$, $gk_{mn}$ dominates the sum, the mode is a gravity wave, and when $k_{mn}^3\sigma/\rho$ dominates it is a capillary wave. In the present study we used a circular cylinder of radius R=5cm, filled with FC-72 to a depth h=8cm such that $\tanh\left(k_{01}h\right)\cong 1$ as used by Das and Hopfinger [5]. Thus the deep water condition is attained, *h/R* >1. The natural frequency for the axisymmetric mode $\omega_{01}$ =27.4719 rad/s. A detailed theory of different sloshing mode and the shape of wave modes for different tank geometries can be found in Ibrahim [10]. The following numerical simulation is done using FC-72 as the liquid of kinematic viscosity $\nu$=0.00406cm$^2$/s, interfacial surface tension $\sigma$ =11dyn/cm and density $\rho$=1690 kg/m$^3$ at 293K.

## 3. Computational method

The computational domain is a cylindrical container with FC-72 at bottom and air at top. At the bottom wall we impose the moving boundary and at the cylindrical inner surface no slip condition is applied. The contact angle has been set to 1. The dimensions of the cylinder are radius *R*=5cm and the height 20cm, filled up to a depth *h*=8cm such that *h/R*=1.6. The simulations have been done in ANSYS 15.0. Mesh has been generated in ICEM CFD and for the fluid flow part FLUENT has been used. Both axisymmetric and three dimensional simulations are done for the axisymmetric mode (01). Volume of fluid (VOF) model is used for multiphase modelling. In phase interactions, a formulation of the Continuum surface force (CSF) model is used in conjunction with wall adhesion, where the surface curvature is computed from local gradients in the surface normal at the interface. The interfacial surface tension is set to be $\sigma$ = 0.011 N/m and the contact angle is taken 1 (FC-72 is fully wetting). Geo-reconstruct scheme is used for tracking the interface. Axisymmetric simulations are done in the stable wave regime and subcritical wave breaking region where pure axisymmetric wave exists. Complete three dimensional simulations are done in the chaotic region and in unstable wave region. Three dimensional simulations are also carried out in the wave breaking and stable wave regions to ensure their axisymmetric nature.

The grid independence test is shown in figure 1. It can be observed from the plot that respectively 21063 and 105336 cells are sufficient for axisymmetric and 3D simulations. We have chosen *A/R*=0.005 and run the simulation for 3-D case to trace the minimum frequency of instability threshold. Similarly for the two dimensional axisymmetric case we fixed the amplitude ratio as 0.012 and searched the minimum frequency of wave appearance. We have also performed time step independence study and it results in optimum time step size of 0.001s. A different grid is used for the analysis of jet formation, the

mesh is chosen based on the last wave amplitude for axisymmetric case (75803 cells) to resolve the jet velocity as accurate as possible. Near the axis mesh is fine and away from axis coarse mesh has been used. The time step used in jetting analysis is 0.0001s.

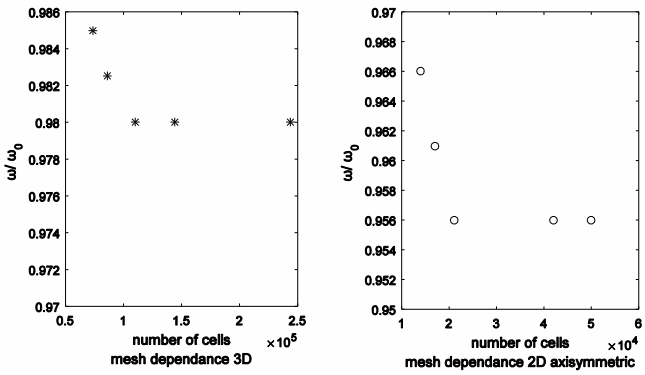


**Figure 1.** the lowest $\omega/\omega_0$ at which the wave appears is plotted against no of cells, for three dimensional case $A/R$=0.005 and for axisymmetric case $A/R$=0.012.

## 4. Results and Discussions

In this section we discuss the results obtained from numerical simulation of axisymmetric gravity waves in the circular container filled with FC72 up to a depth of $h$=8cm. Throughout the following discussion amplitude corresponds to the non-dimensional amplitude $A/R$ and frequency $\omega/\omega_0$, where $\omega$ is the wave frequency and $\omega_0$ is the natural frequency of 01 mode.

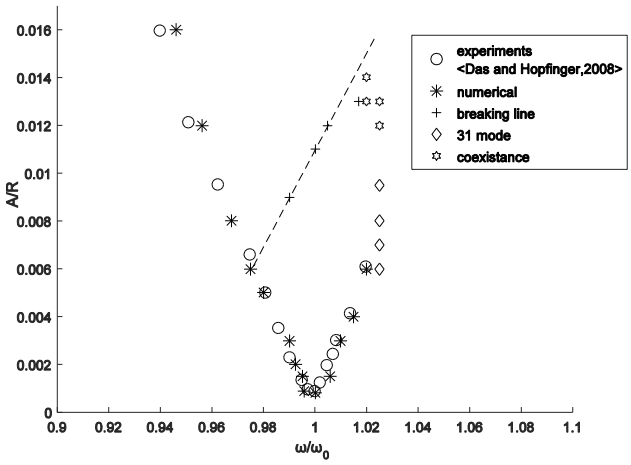


**Figure 2.** Instability threshold obtained from numerical simulations (*) is compared with experimental results [5]. + shows the region where the wave grows exponentially and breaks. The symbols × and ◊ show the regions for 31 mode and coexistence of 31 and axisymmetric modes respectively. The wave mode for the latter is initially axisymmetric and then coexists with the 31 mode.

### *4.1. Instability threshold*

The dimensionless forcing amplitude as a function of frequency ratio in figure 2 shows the instability threshold for wave appearance and also breaking limit for stable waves. The numerical results show a very good agreement with the experimental results of Das and Hopfinger [5]. The instability threshold indicates required minimum forcing at which waves appear at the interface. Whereas the breaking line shows the region above which the waves will grow exponentially and break as the steepness limited

criteria is reached and below the line waves unstable wave motions are observed. In a given range of forcing amplitude (lower that unstable wave and higher than instability threshold) stable waves are observed. The axisymmetric mode 01 lies in the frequency band $\omega/\omega_0 = 0.945$ to $\omega/\omega_0 = 1.025$, and then it follows the 31 mode.

*4.2. Amplitude modulations*

From the simulation results different types of wave motions are observed in different regimes of the instability diagram (figure 2). Important observations here are the different time scales of wave amplitude modulations. Wave amplitude modulation happens by slow time scale, period tripling and period quadrupling. In some portion of the unstable wave motion (subcritical regime) regime period tripling (here for $A/R = 0.005$) has been observed whereas some part (supercritical regime) shows period quadrupling behavior (here at $A/R$=0.010).

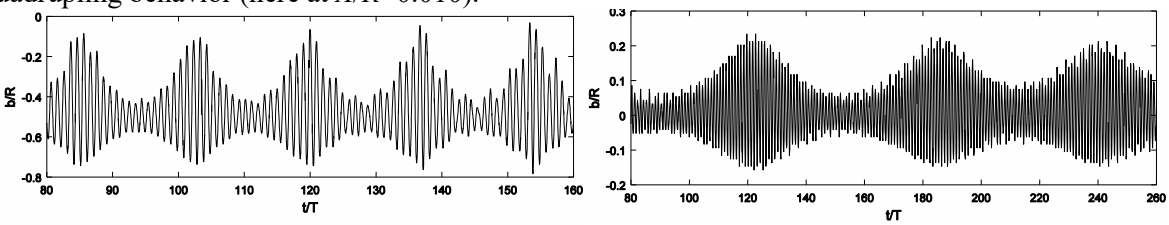


*(a) A/R*=0.012 *(b) A/R*=0.0025

**Figure 3.** Comparison of slow time scale amplitude modulation for different forcing amplitudes ($A/R$=0.012 and 0.0025). Here $b$ is the wave amplitude.

In figure 3 the wave amplitudes are plotted as a function of dimensionless time $t/T$, where $T=2\pi/\omega$. Figure shows amplitude modulation occurring in slow time scale for $A/R$=0.012 and $A/R$=0.0025 with half period growth in t/T = 63 and 17 respectively. Period of the amplitude modulation decreases with increase in forcing amplitude which is consistent with the slow time similar to Miles [2]. Period tripling is observed at $\omega/\omega_0 = 0.985$, $A/R$=0.005, where the steep wave crest is seen followed by a flat crest and a slightly higher amplitude wave (figure 4). This instability is also observed with slight

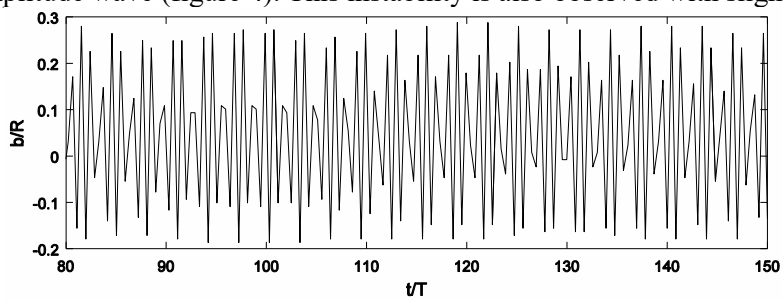


**Figure 4.** Period tripling cycle, $A/R$=0.005 and $\omega/\omega_0 = 0.985$, the shorter waves are flat crested and the higher waves appeared with steep crests.

demodulation where the wave initially has an amplitude modulation and eventually shifts to period tripling. In the unstable wave region for $A/R$=0.005 and $\omega/\omega_0 = 0.9825$, the wave crest is formed slightly off the center and it rotates about the axis of the cylinder. The rotation is observed when the simulation is continued for a longer period of time. Here after $t/T$=350 rotation starts. Figure 5 shows the images of wave crest for one complete rotation. For $A/R$=0.010 $\omega/\omega_0 = 1.02$, period quadrupling event is observed which is similar to the above mentioned period tripling event (figure 6) at frequencies higher than the natural frequency and in the close proximity of the 31 mode but in the unstable wave motion regime. Below the breaking line, $\omega/\omega_0 = 1.017$, $A/R$=0.01275 the wave initially shows an amplitude modulation and then slowly demodulate by shrinking the time period of modulation and increasing the amplitude. In some cases at slightly higher amplitude for a given frequency, the wave amplitude demodulates and the wave breaks very near the breaking line for $A/R$=0.013, $\omega/\omega_0 = 1.017$. This can be

explained as demodulation causes increase in the wave height and wave breaks by deep water wave breaking mechanism.

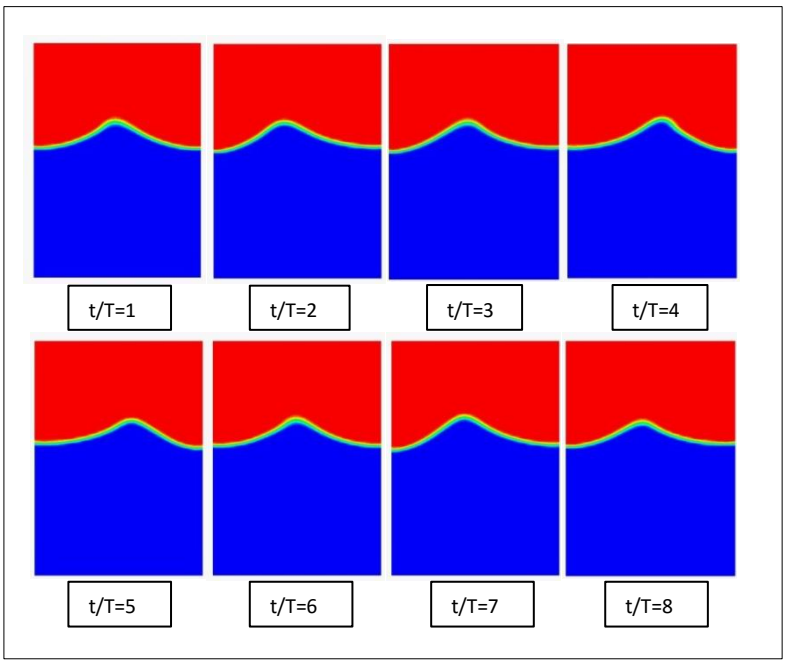


**Figure 5.** Rotation for $A/R$=0.005, $\omega/\omega_0$= 0.9825 , the time evolution of crest of the wave is shown.

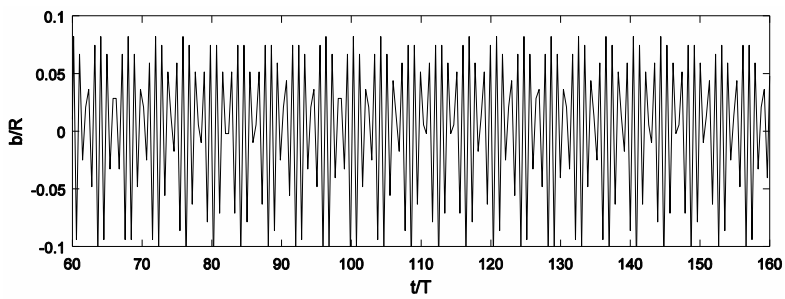


**Figure 6.** Wave pattern observed near breaking $A/R$= 0.010 and $\omega/\omega_0$= 1.02, it can be seen that each wave packet of envelope carries four waves of the signal

*4.3. Coexistence*

The axisymmetric mode exists in the range $\omega/\omega_0$ = 0.94 to $\omega/\omega_0$ = 1.025, for amplitude $A/R$=0.006 and $\omega/\omega_0$ = 1.025 shifts to 31 mode. As the amplitude is slowly increased from $A/R$=0.006 to 0.015 with fixed frequency $\omega/\omega_0$ = 1.025 pure 31 mode is seen till 0.012. Above a critical forcing amplitude ($A/R$ = 0.012) coexistence of 01 and 31 modes is observed. Effect of both the modes is substantial to result in a different type of wave pattern. For $A/R$=0.014 and 0.013 $\omega/\omega_0$ = 1.02 the 01 and 31 mode exists together and the wave breaking occurs only on the 31 mode showing dominance of 31 mode. As in figure 7, $A/R$=0.01225, $\omega/\omega_0$ = 1.020, the crest at center is the wave form for axisymmetric mode and the crest in 3 location at the edge is of 31 mode.

*4.4. Jet formation*

When $A>A_{breaking,}$ the wave breaking occurs for axisymmetric mode. The breaking line for this mode has been traced numerically and is shown in instability threshold diagram (figure 2). The deep water wave

breaking due to steepness limited criteria $H/L$=0.142 (for gravity waves in laterally unbounded cases), where $H$ is the peak to peak height and $L$ is the wave length. The maximum steepness numerically obtained is, $H/L$=0.30 at $A/R$=0.016, $\omega/\omega_0$ = 0.985.

**Figure 7.** Coexistence of 01 and 31 mode ($A/R$=0.01225, $\omega/\omega_0$ = 1.02).

In the breaking region, exponential growth of amplitude and breaking occurs with the high velocity jet ejection from the fluid interface due to the inertial collapse as observed by previous investigators [5, 11]. The jetting may occur with or without pinch-off. A representative case is shown in figure 8 for $A/R$=0.016 and $\omega/\omega_0$ = 0.995. Here the jet forms with a bubble pinch-off. Jet velocity is measured at a specific point in the path of the jet, the instant at which jet passes the chosen point shows the peak value corresponds to the velocity of jet at that instant. In the breaking region waves are recorded with high steepness $H/L$>0.3 and the maximum jet velocity is found to be 12m/s in the simulations performed here. The jet velocity depends on the shape of the cavity formed before collapse which also depends on the viscosity and surface tension of the working fluid.

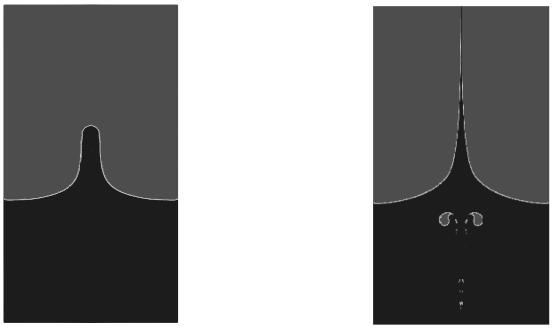

*(a)* last stable wave amplitude *(b)* jetting

**Figure 8.** Images showing the last wave amplitude ($t=t_0$) before collapse and the jetting ($t=t_0$+0.2 s) ($A/R$=0.016 with, $\omega/\omega_0$ = 0.995).

## 5. Conclusion

The numerically simulated stability threshold diagram for axisymmetric gravity wave (01 mode) in a circular cylinder for low viscosity and low surface tension fluid (FC72) with infinite liquid depth shows good agreement with the reported experimental investigations. Bifurcation to 31 mode and coexistence with 31 mode of this axisymmetric mode has been found. Amplitude demodulation has been observed near the breaking and the demodulation forms stable wave height.The period tripling event matches with the earlier observations [3, 5]. Wave amplitude modulations occurs at different time scale (slow, period tripling and period quadrupling) without breaking. When the forcing amplitude crosses a critical limit at a given frequency, inertial collapse of the wave trough causes a high velocity jet ejection from the liquid surface with or without pinch-off. The jet velocity obtained from simulation agrees well with the experimental results for same fluid under similar conditions.

**References**

[1] Benjamin T B & Ursell F1954 The stability of plane free surface of a liquid in a vertical periodic motion. *Proc. R. Soc. Lond. A* **225** 505–515.
[2] Miles J W 1984 Parametrically excited solitary waves *J . Fluid Mech*. **148** 451-460.
[3] Jiang L, Ting C-L, Perlin M & Schultz W W 1996 Moderate and steep Faraday waves:instabilities, modulation and temporal asymmetries *J. Fluid Mech.* **329** 215-301.
[4] Royon-Lebeaud A, Hopfinger EJ & Cartellier A 2007 Liquid sloshing and wave breaking in circular and square-base cylindrical containers *J. Fluid Mech* **577** 467-494.
[5] Das S P & Hopfinger E J 2008 Parametrically forced gravity waves in circular cylinder and finite time singularity *J. Fluid Mech.* **599** 205–228.
[6] Faltinsen O M, Rognebakke O F & Timokha A N 2003 Resonant three-dimensional nonlinear sloshing in a square-base basin. *J. Fluid Mech*. **487** 1–42.
[7] Miles J W 1984 Nonlinear Faraday resonance *J . Fluid Mech*. **146** 285-302.
[8] Nicolas P, Damir J & Tuckerman L S 2009 Numerical simulation of faraday waves *J. Fluid Mech*. **635** 1-26.
[9] Peilong Chen & Kuo-An Wu 2000 Subcritical bifurcations and nonlinear balloons in faraday waves *Phys.Rev.Lett*.**85**.3813.
[10] Ibrahim R A 2005 Liquid sloshing dynamics *Cambridge University Press*.
[11] Zeff BW, Kleber B, Fineberg J & Lathrop D P 2000 Singularity dynamics in curvature collapse and jet eruption on a fluid surface *Nature* **403** 401–404.